Analytica Chimica Acta 894 (2015) 85–90

Contents lists available at ScienceDirect

Analytica Chimica Acta

journal homepage: www.elsevier.com/locate/aca

Fluorescence imaging for in situ detection of cell surface sialic acid by competitive binding of 3-(dansylamino)phenylboronic acid

Ruocan Qian, Lin Ding, Liwen Yan, Huangxian Ju*

State Key Laboratory of Analytical Chemistry for Life Science, School of Chemistry and Chemical Engineering, Nanjing University, Nanjing, 210093, PR China

HIGHLIGHTS

- An off–on switchable fluorescence nanoprobe to recognize sialic acid was constructed.
- The competition between cell surface sialic acid and PSA lights up the fluorescence.
- The competitive method can be used for in situ imaging of cell surface sialic acid.
- The imaging method can detect cell number and the amount of cell surface sialic acid.
- This method can be used for the dynamic monitoring of cell surface SA change.

GRAPHICAL ABSTRACT

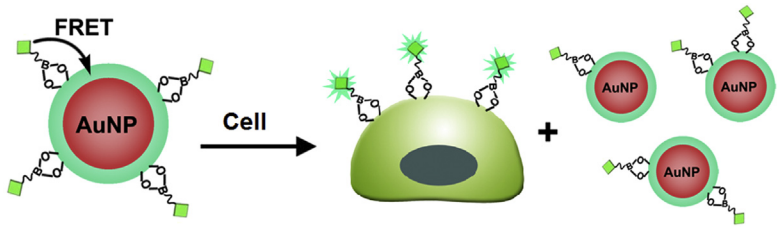

ARTICLE INFO

Article history:
Received 22 March 2015
Received in revised form
25 August 2015
Accepted 27 August 2015
Available online 3 September 2015

Keywords:
Cell imaging
Fluorescence resonance energy transfer
Sialic acid
Gold nanoparticles
3-(Dansylamino)phenylboronic acid
In situ monitoring

ABSTRACT

Sialic acid (SA) usually locates at the terminal position of the sugar chains on cell membranes, and its expression level is closely associated with cancer. Here polysialic acid (PSA) embedded gold nanoparticles (AuNPs) were prepared and functionalized with fluorescent 3-(dansylamino)phenylboronic acid (DAPB) for in situ imaging and detection of cell surface SA. The fluorescence resonance energy transfer (FRET) from DAPB to AuNPs quenched the fluorescence of DAPB. In the presence of additional SA or SA-abundant cells, the competitive binding of DAPB with SA and PSA led to the release of the assembled DAPB from the surface of PSA-embedded AuNPs, resulting in fluorescence of DAPB on SA-abundant cell surface. The proposed methods realized the in situ imaging and monitoring of cell surface SA, and could also be applied to the quantification of cell number and the amounts of cell surface SA. This work not only proposed a convenient visualization method for the analysis of SA on cell membranes, but also provided a potential tool for accelerating the elucidation of the basic role of SA in various biological processes and development of anti-cancer therapies.

1. Introduction

Sialic acids (SAs), also called N-acetyl neuraminic acid, include a family of 9-carbon acidic monosaccharides, and can usually be found at the terminal end of the glycan chains on cell surface [1]. In the body of vertebrates, SAs participate in various physiological and pathological processes, such as intracellular signaling and cell recognition [2]. The change of the expression level of cell surface SA is closely related to the development of cancer, as high expression

* Corresponding author.
E-mail address: hxju@nju.edu.cn (H. Ju).

http://dx.doi.org/10.1016/j.aca.2015.08.054
0003-2670/

of SA can usually be found on tumor cell surface [3]. Therefore, the detection of cell surface SA, especially in situ analysis, is of great significance to the diagnosis and therapy of cancer.

Traditional labeling detection methods commonly use different types of lectins to recognize the corresponding glycans [4–7]. Both the number of glycan–lectin pairs and the specificity of glycan–lectin recognition have been known to be unsatisfactory [8,9]. Thus the exploration of high specific recognition mechanism for selective glycan analysis is in urgent need by cancer researchers. Recent research has suggested that SA can specifically combine with phenyl boronic acids though a reversible boronic acid–diol interaction at normal physiological pH condition (7.4) [10,11]. The reversible linkage of boronic acid with SA offers a brand-new direction for the recognition and detection of cell surface SA by assembling the boronic groups on various biosensing materials [12–15].

Recently, a large number of biosensing materials have been designed for cell analysis with desirable performance [16–18]. Gold nanoparticles (AuNPs) are especially attractive in cytosensing due to the favorable biocompatibility and ease of functionalization [19–24]. Moreover, the AuNPs can be extensively used as not only the carriers of signal molecules [9,19–24], but also the quencher of some fluorescent dyes [25–27] or quantum dots [28,29] via fluorescence resonance energy transfer (FRET). This work integrated the quenching ability of AuNPs on the fluorescence of dansyl group [19] with the recognition ability of boronic group to SA [10–15] to design a novel nanoprobe, which could be prepared by assembling 3-(dansylamino)phenylboronic acid (DAPB) on polysialic acid (PSA) embedded AuNPs (PSA-AuNPs). The fixed DAPB could be released in the presence of SA or SA-abundant cells, due to the competitive binding of DAPB with SA or cell surface SA and PSA. Thus the fluorescence of DAPB on SA-abundant cell surface could be turned on to provide a visualization method for in situ imaging of cell surface SA (Scheme 1). The practicality of the imaging method was confirmed by its application in quantification of cell number and the amounts of cell surface SA. In addition, this strategy realized in site monitoring of SA expression level on cell surface, which may offer a potential tool for the development of SA-targeted anticancer methods.

2. Experimental

2.1. Chemicals

Chloroauric acid ($HAuCl_4 \cdot 4H_2O$) was obtained from Shanghai Chemical Reagent Company (China). Trisodium citrate was obtained from Sinopharm Chemical Reagent Co., Ltd. (China). DAPB, PSA, SA and sialidase were purchased from Sigma–Aldrich Inc. (USA). D282 dye for staining cell membrane was from Invitrogen Co. Ltd (Shanghai, China). HeLa cells (cervical cancer cell) were from KeyGen Biotech. Co. Ltd. (Nanjing, China). Phosphate buffer saline (PBS, pH 7.4) contained 136.7 mM NaCl, 2.7 mM KCl, 8.72 mM Na_2HPO_4, and 1.41 mM KH_2PO_4. All aqueous solutions were prepared using ultrapure water (≥18 MΩ, Milli-Q, Millipore).

2.2. Apparatus

The transmission electron microscopic (TEM) images were obtained on a JEM-2100 transmission electron microscope (JEOL Ltd., Japan). Dynamic light scattering (DLS) was observed on a 90 Plus/BI-MAS equipment (Brook haven, USA). The UV–vis absorption spectra were obtained with a UV–vis spectrophotometer (Nanodrop-2000C, Nanodrop, USA). The fluorescence spectra were obtained on a spectrofluorophotometer (RF-5301PC, Shimadzu, Japan). The cell images were gained on a TCS SP5 laser scanning confocal microscope (Leica, Germany). MTT assay was performed on a microplate reader (680, Bio-Rad, USA).

2.3. Cell culture and treatment

HeLa cells were cultured in a flask in Dulbecco's modified Eagle's medium (DMEM, GIBCO) supplemented with 10% fetal calf serum (FCS, Sigma), penicillin (100 μg mL^{-1}), and streptomycin (100 μg mL^{-1}) at 37 °C in a humidified chamber, containing 5% CO_2. Cell number was determined using a Petroff-Hausser cell counter (USA).

2.4. Preparation of DAPB functionalized PSA-AuNPs as the nanoprobe

PSA-AuNPs were firstly prepared by heating 200 mL $HAuCl_4$ solution (0.01%) containing 30 mg PSA to 100 °C, followed with addition of 5.0 mL trisodium citrate (1%) to the boiling solution under continuous stirring [8]. The reaction mixture was stirred at 100 °C for 1 h until the color turned deep red to obtain PSA-AuNP solution, which was stored at 4 °C. DAPB (0.1 mL, 0.3 mg mL^{-1}) was then added to 1.0 mL of the obtained PSA-AuNP solution and stirred at room temperature overnight. Afterward, the mixture was centrifuged and washed twice with PBS, and the resulting

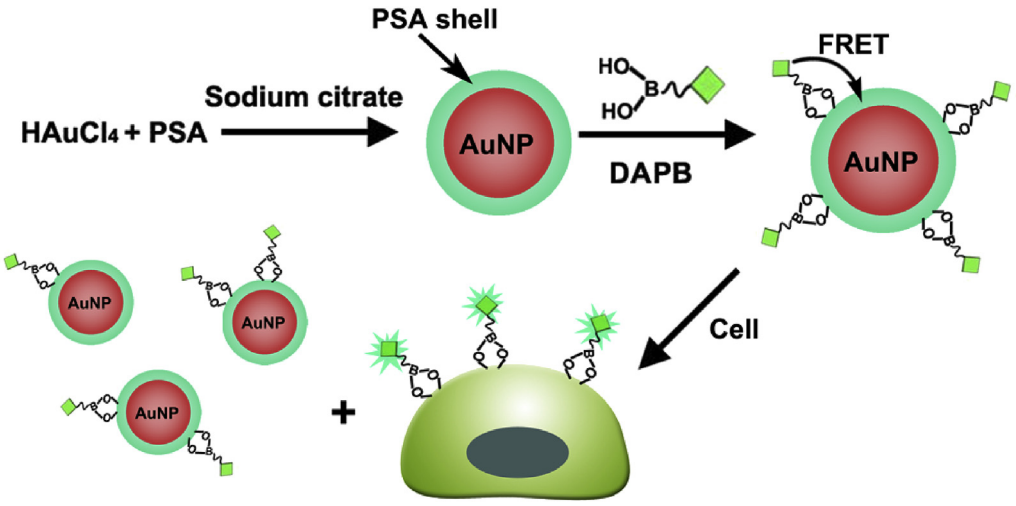

Scheme 1. Schematic illustration of nanoprobe preparation and off–on fluorescence switch for in situ imaging of cell surface SA.

nanoprobe was finally re-suspended in 1 mL PBS. The supernatant containing excess DAPB was collected for fluorescent analysis to determine the amount of DAPB on each functionalized PSA-AuNP. The DAPB functionalized PSA-AuNPs were characterized with TEM, DLS and UV–vis spectroscopy, and the concentration of the nanoprobe solution is calculated to be 1 nM.

2.5. Quantification of HeLa cells with the functional nanoprobe

Nanoprobe solution (1 mL) was mixed with 100 μL cell suspension of different concentrations, respectively. After incubation for 1 h at 37 °C, the fluorescent intensity of the mixtures was determined to obtain the calibration curve.

2.6. In situ imaging of cell surface SAs

HeLa cells (0.5 mL, 1×10^6 mL^{-1}) were seeded in each confocal dish for 24 h, and 100 μL of the proposed nanoprobe was then added into the dish. After 1-h incubation at 37 °C, the cells were sent for confocal observation. For the monitoring of the cell surface SAs under the treatment of sialidase, HeLa cells were treated with sialidase (60 mU) for different times and then incubated with 100 μL nanoprobe for 1 h to perform confocal imaging.

2.7. In situ monitoring and quantification of cell surface SA under sialidase treatment

In order to test the feasibility of the nanoprobe for the in situ monitoring of cell surface SA, sialidase, an enzyme that cleave the terminal SA residues from the glycan chains, was used to treat the cells. Briefly, HeLa cells were treated with sialidase for different times to show different cell surface SA expression levels, which provided the standard samples to obtain the calibration curve for quantification. Afterward, the sialidase-treated cells were split into two groups. The first group was used for confocal imaging, and the cells were incubated with 100 μL nanoprobe (DAPB functionalized PSA-AuNPs) to obtain the average fluorescence intensity of the cell area (*FIC*, which is defined as the average blue channel intensity in cell area read by Adobe Photoshop software, subtracted by background blue channel intensity at the wavelength of 450 nm). Another group was used to calculate the amount of cell surface SA with a standard curve for fluorescence measurement of DAPB. These cells were centrifuged, redistributed in 100 μL PBS, and then added to 1 mL nanoprobe solution. After 1-h incubation at 37 °C, the fluorescence intensity was determined, respectively, to obtain the amounts of the DAPB released from AuNPs. Assuming the interaction between DAPB and SA possessed one-to-one correspondence, the number of SA (n) on each HeLa cell could be obtained. From the plot of *FIC* vs. n, the semi-quantitative estimation of the average number of cell surface SA under sialidase treatment was achieved.

3. Results and discussion

3.1. Characterization of PSA-AuNPs and nanoprobe

The transmission electron microscopic (TEM) image of the PSA-AuNPs showed an average diameter of 18 ± 2.3 nm ($n = 32$) with a narrow distribution, which was consistent with the dynamic light scattering (DLS) result of 20.2 nm and 5 nm larger than the naked AuNPs synthesized under the same condition without the presence of PSA (Fig. S1a–S1c, Supplementary material). The average diameter of PSA-AuNPs obviously increased with an apparent core–shell structure. The UV–vis absorption spectrum of PSA-AuNPs showed an absorption peak at 528 nm, which red shifted to 537 nm after DAPB was conjugated on their surface (Fig. S1d, Supplementary material), confirming the successful modification of DAPB. The average amount of DAPB assembled on each nanoprobe was measured to be around 10^4 (Fig. S2, Supplementary material).

3.2. Fluorescence of DAPB after competitive binding with SA monosaccharides or HeLa cells

SA monosaccharides and HeLa cells with overexpressed SA on the surface of cell membrane were used for evaluating the competition-based fluorescence recovery of the DAPB. No fluorescence of the nanoprobe solution could be observed in the absence of SA or HeLa cells (curve A in Fig. S3a and S3b, Supplementary material), indicating the quenching effect of the AuNP core to DAPB fluorescence. The tiny fluorescence occurred at a long time resulted from the dissociation of DAPB from the nanoprobe surface. In the presence of SA or HeLa cells, the solution showed gradually increasing fluorescence of DAPB, which tended to a maximum value after 1 h (curve B in Fig. S3a and S3b, Supplementary material), indicating the competitive binding of DAPB with free SA or cell surface SA and the PSA-AuNPs, which led to the release of DAPB from nanoprobe surface. This result demonstrated the competition mechanism of the fluorescence recovery and an efficient method for in situ fluorescence imaging of cell surface SA.

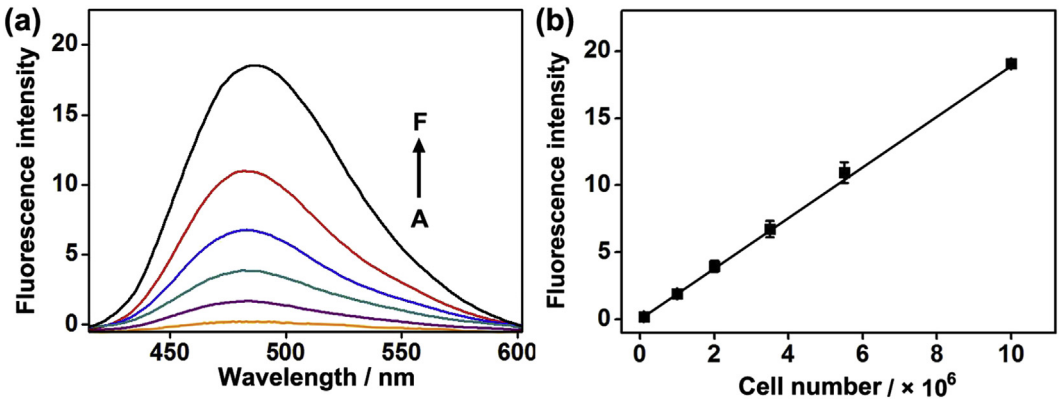

Fig. 1. (a) Fluorescence spectra of nanoprobe solution (1 mL, 1 nM) after treated with 1.0×10^5, 1.0×10^6, 2.0×10^6, 3.5×10^6, 5.5×10^6 and 1.0×10^7 HeLa cells for 1 h (from A to F). (b) Plot of fluorescence intensity *vs.* cell number.

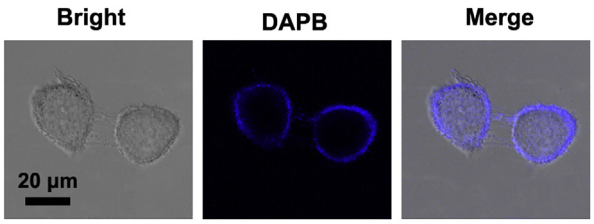

Fig. 2. Confocal images of HeLa cells incubated with nanoprobe solution.

3.3. Fluorescence detection of HeLa cells

The proposed nanoprobe was firstly used for the quantification of HeLa cells. After HeLa cells were incubated with the nanoprobe solution (1 mL) for 1 h, the fluorescence intensity (I) of the mixtures with different numbers of cells (C) was detected to obtain the calibration curve (Fig. 1). The plot of I vs. C showed a linearity with a correlation coefficient R of 0.995. At the points of 1.0×10^5 and 1.0×10^7 cells, the fluorescence signals showed the relative standard deviation of 7.2% and 3.6% for six determinations, respectively, indicating good reproducibility for cell quantification.

Assuming the fluorescence of free DAPB was identical with the DAPB bound to free SA or cell surface SA, the amount of the DAPB released from AuNPs to bind free SA or cell surface SA could be obtained (Fig. S2, Supplementary material), which provided a fluorescence method for in situ detection of cell surface SA. The average number of SA molecules (n) on the surface of each HeLa cell could be calculated to be about 7.0×10^8.

3.4. Cytotoxicity of DAPB functionalized PSA-AuNPs

Before cell imaging analysis, the cytotoxicity of DAPB functionalized PSA-AuNPs was evaluated by MTT assay. HeLa cells maintained high viability during the 3-h incubation (Fig. S4, Supplementary material), exhibiting satisfactory biocompatibility.

3.5. In situ imaging analysis of cell surface SA

For in situ imaging analysis of cell surface SA, HeLa cells were used as the model to perform the confocal imaging detection. HeLa cells (0.5 mL, 1×10^6 mL^{-1}) were firstly seeded in a 20 mm confocal dish and incubated for 24 h. After 1-h incubation of HeLa cells with 100 μL nanoprobe solution, the dish was sent for observation under the confocal microscope (Fig. 2). The fluorescent image showed obvious fluorescence signal of DAPB, which was completely distributed on the membrane of HeLa cells. While the region of cytoplasm showed negligible fluorescence, indicating the specific recognition of DAPB with the cell surface SA. Thus the proposed nanoprobe possessed good affinity and specificity with negligible background signal. This was obviously different from the observation of HeLa cells directly treated with DAPB solution, which showed the fluorescence signal of DAPB not only on the cell membrane but also in the cytoplasm due to the unspecific endocytosis of DAPB (Fig. S5, Supplementary material). Thus the nanoprobe could not be taken in by the cells, and the signal came from the competitive binding of the SA on cell surface with those on PSA-AuNPs. This provided another method for imaging cell surface SAs with a low background.

3.6. Monitoring and quantification of cell surface SA in response to sialidase

The imaging method for the monitoring of the change of cell surface SA was demonstrated by using a SA-related enzyme, sialidase, to treat HeLa cells, and then using the proposed nanoprobe to incubate the enzyme-treated cells for confocal observation. The sialidase treatment could cut SA molecules down from the terminal of glycan chains, which reduced the intensity of fluorescence signal in the confocal images. After HeLa cells (0.5 mL, 1×10^6 mL^{-1}) were cultured with sialidase (60 mU) in a confocal dish for different times, the fluorescence intensity of DAPB on sialidase-treated HeLa cells obviously decreased (Fig. 3). After 4-h treatment with

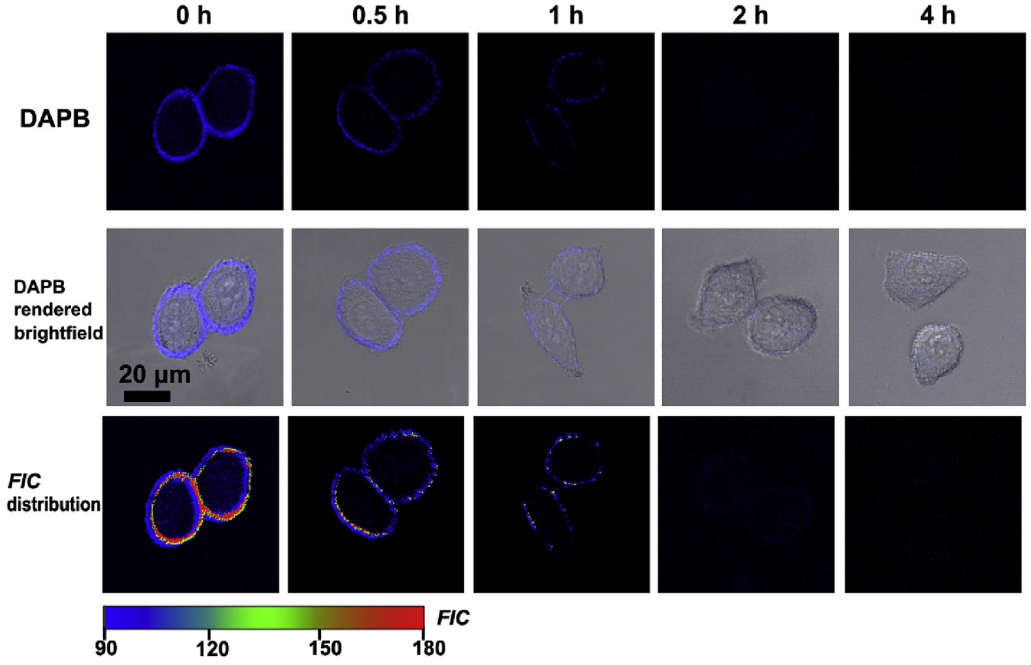

Fig. 3. Confocal images of HeLa cells treated with sialidase (60 mU) for different times and then incubated with nanoprobe solution (100 μL, 1 nM) for 1 h. The fluorescent images were color-coded by a pseudocolor processing system to show the distribution of SAs. (For interpretation of the references to color in this figure legend, the reader is referred to the web version of this article.)

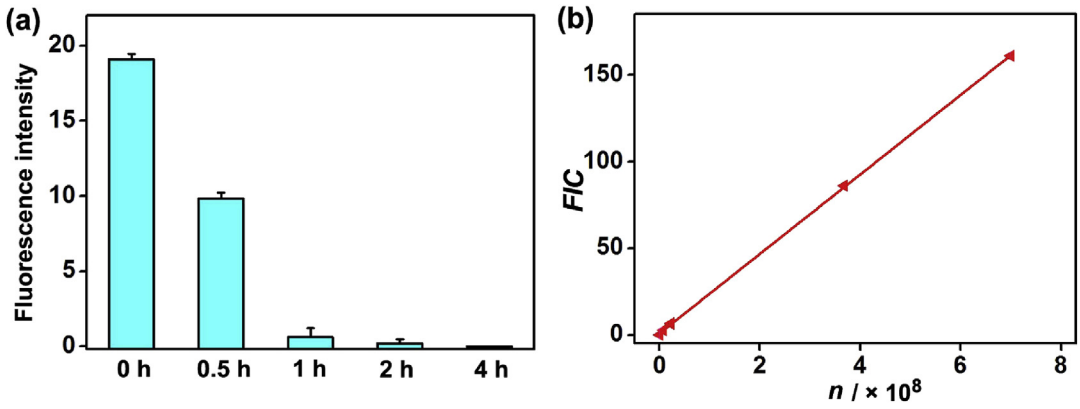

Fig. 4. (a) Plot of fluorescence intensity in vitro vs. sialidase treatment time. (b) Plot of *FIC vs. n* (number of SA molecules).

sialidase, no fluorescence signal could be detected. The control experiment without sialidase-treatment did not show the decrease of DAPB fluorescence on the cell surface (Fig. S6, Supplementary material). Therefore, sialidase exhibited efficient cleavage of cell surface SA. These results demonstrated the ability of the proposed method for noninvasive detection of the expression levels of cell surface SA, which provided a potential tool for the researching of SA-targeted anti-cancer methods.

Afterward, the assessment of the cell surface SA with the DAPB functionalized PSA-AuNPs for imaging assay was further examined. As mentioned above, after HeLa cells were treated with sialidase for different times, they possessed different SA expression levels, thus providing the standard samples for getting the calibration curve. The sialidase-treated HeLa cells were divided into two groups. One group was incubated with nanoprobe to obtain the average fluorescence intensity of the cell area (*FIC*) from the confocal images (Fig. 3) by reading the average blue channel intensity within cell area (subtracted by background blue channel intensity) with Adobe Photoshop software, while another group was used to obtain the corresponding SA number *n* on each cell via the standard curve for the calculation of DAPB amount (Fig. S2, Supplementary material). These cells were added to 1 mL nanoprobe solution, and incubated for 1 h to perform the fluorescence detection (Fig. 4a). The calibration curve was shown in Fig. 4b, which showed a linear relationship between the *FIC* and *n*. With this calibration curve, the average number of cell surface SA could be estimated by reading the *FIC* value from the confocal fluorescence images, which was quite simple and convenient, compared with traditional methods. The average amount of SA on each HeLa cell was detected to be 7.0×10^8, and the number of cell surface SA sharply decreased from original 7.0×10^8 to 6.0×10^4 after treated with sialidase for 0.5 h.

4. Conclusions

This work prepared DAPB functionalized PSA-AuNPs for in situ imaging and fluorescence quantification of cell surface SA by the competitive binding of DAPB to PSA-AuNPs and cell surface SA, which turned on the fluorescent signal of the DAPB on cell surface. The proposed approach showed good performance for the detection of cell number, and realized the imaging of cell surface SA with low background. This method could be applied for the monitoring of cell surface SA at a certain time point. Compared with existed methods, the proposed strategy used a dual functional molecule to achieve both the FRET from DAPB to AuNPs and the specific recognition of boronic group to SA and provided a convenient visualization method for in situ imaging of cell surface SA via a one-step incubation. We anticipated that the proposed protocol would be favorable for the elucidation of SA-involved biological processes, the diagnosis of cancer and the development of SA-targeted anti-cancer strategies.

Acknowledgments

This work was financially supported by the National Basic Research Program (2014CB744501), National Natural Science Foundation of China (91413118, 91213301, 21135002, 21322506, 21121091).

Appendix A. Supplementary data

Supplementary data related to this article can be found at http://dx.doi.org/10.1016/j.aca.2015.08.054.

References

[1] S. Hakomori, Tumor malignancy defined by aberrant glycosylation and sphingo(glyco)lipid metabolism, Cancer Res. 56 (1996) 5309–5318.
[2] D.H. Dube, C.R. Bertozzi, Glycans in cancer and inflammation. Potential for therapeutics and diagnostics, Nat. Rev. Drug Discov. 4 (2005) 477–488.
[3] A. Varki, Sialic acids in human health and disease, Trends Mol. Med. 14 (2008) 351–360.
[4] L. Ding, W. Cheng, X.J. Wang, Y.D. Xue, J.P. Lei, Y.B. Yin, H.X. Ju, A label-free strategy for facile electrochemical analysis of dynamic glycan expression on living cells, Chem. Commun. (2009) 7161–7163.
[5] L. Ding, Q.J. Ji, R.C. Qian, W. Cheng, H.X. Ju, Lectin-based nanoprobes functionalized with enzyme for highly sensitive electrochemical monitoring of dynamic carbohydrate expression on living cells, Anal. Chem. 82 (2010) 1292–1298.
[6] X.A. Zhang, Y.Q. Teng, Y. Fu, L.L. Xu, S.P. Zhang, B. He, C.G. Wang, W. Zhang, Lectin-based biosensor strategy for electrochemical assay of glycan expression on living cancer cells, Anal. Chem. 82 (2010) 9455–9460.
[7] J.J. Kohler, Aniline: a catalyst for sialic acid detection, ChemBioChem 10 (2009) 2147–2150.
[8] L. Ding, R.C. Qian, Y.D. Xue, W. Cheng, H.X. Ju, *In situ* scanometric assay of cell surface carbohydrate by glyconanoparticle-aggregation-regulated silver enhancement, Anal. Chem. 82 (2010) 5804–5809.
[9] W. Cheng, L. Ding, J.P. Lei, S.J. Ding, H.X. Ju, Effective cell capture with tetrapeptide-functionalized carbon nanotubes and dual signal amplification for cytosensing and evaluation of cell surface carbohydrate, Anal. Chem. 80 (2008) 3867–3872.
[10] H. Otsuka, E. Uchimura, H. Koshino, T. Okano, K. Kataoka, Anomalous binding profile of phenylboronic acid with N-acetylneuraminic acid (Neu5Ac) in aqueous solution with varying pH, J. Am. Chem. Soc. 125 (2003) 3493–3502.
[11] X. Wu, Z. Li, X.X. Chen, J.S. Fossey, T.D. James, Y.B. Jiang, Selective sensing of saccharides using simple boronic acids and their aggregates, Chem. Soc. Rev. 42 (2013) 8032–8048.
[12] A.P. Liu, S. Peng, J.C. Soo, M. Kuang, P. Chen, H.W. Duan, Quantum dots with phenylboronic acid tags for specific labeling of sialic acids on living cells, Anal. Chem. 83 (2011) 1124–1130.
[13] A. Matsumoto, N. Sato, K. Kataoka, Y. Miyahara, Noninvasive sialic acid detection at cell membrane by using phenylboronic acid modified self-assembled monolayer gold electrode, J. Am. Chem. Soc. 131 (2009) 12022–12023.

[14] A. Matsumoto, H. Cabral, N. Sato, K. Kataoka, Y. Miyahara, Assessment of tumor metastasis by the direct determination of cell-membrane sialic acid expression, Angew. Chem. Int. Ed. 49 (2010) 5494–5497.
[15] E. Han, L. Ding, H.X. Ju, Highly sensitive fluorescent analysis of dynamic glycan expression on living cells using glyconanoparticles and functionalized quantum dots, Anal. Chem. 83 (2011) 7006–7012.
[16] Y.F. Wu, H. Zhou, W. Wei, X. Hua, L.X. Wang, Z.X. Zhou, S.Q. Liu, Signal amplification cytosensor for evaluation of drug-induced cancer cell apoptosis, Anal. Chem. 84 (2012) 1894–1899.
[17] J.L. Vivero-Escoto, I.I. Slowing, C.W. Wu, V.S.Y. Lin, Photoinduced intracellular controlled release drug delivery in human cells by gold-capped mesoporous silica nanosphere, J. Am. Chem. Soc. 131 (2009) 3462–3463.
[18] I. Slowing, B.G. Trewyn, V.S.Y. Lin, Effect of surface functionalization of MCM-41-type mesoporous silica nanoparticles on the endocytosis by human cancer cells, J. Am. Chem. Soc. 128 (2006) 14792–14793.
[19] A. Llevot, D. Astruc, Applications of vectorized gold nanoparticles to the diagnosis and therapy of cancer, Chem. Soc. Rev. 41 (2012) 242–257.
[20] B. Duncan, C. Kim, V.M. Rotello, Gold nanoparticle platforms as drug and biomacromolecule delivery systems, J. Control Release 148 (2010) 122–127.
[21] F. Li, H.Q. Zhang, B. Dever, X.F. Li, X.C. Le, Thermal stability of DNA functionalized gold nanoparticles, Bioconjugate Chem. 24 (2013) 1790–1797.
[22] E. Boisselier, D. Astruc, Gold nanoparticles in nanomedicine: preparations, imaging, diagnostics, therapies and toxicity, Chem. Soc. Rev. 38 (2009) 1759–1782.
[23] D.A. Giljohann, D.S. Seferos, P.C. Patel, J.E. Millstone, N.L. Rosi, C.A. Mirkin, Oligonucleotide loading determines cellular uptake of DNA-modified gold nanoparticles, Nano Lett. 7 (2007) 3818–3821.
[24] D.S. Seferos, D.A. Giljohann, H.D. Hill, A.E. Prigodich, C.A. Mirkin, Nano-flares: probes for transfection and mRNA detection in living cells, J. Am. Chem. Soc. 129 (2007) 15477–15479.
[25] C.S. Yun, A. Javier, T. Jennings, M. Fisher, S. Hira, S. Peterson, B. Hopkins, N.O. Reich, G.F. Strouse, Nanometal surface energy transfer in optical rulers, breaking the FRET barrier, J. Am. Chem. Soc. 127 (2005) 3115–3119.
[26] F. Gao, P. Cui, X. Chen, Q. Ye, M. Li, L. Wang, A DNA hybridization detection based on fluorescence resonance energy transfer between dye-doped core-shell silica nanoparticles and gold nanoparticles, Analyst 136 (2011) 3973–3980.
[27] J. Chen, Y. Huang, S.L. Zhao, X. Lu, J.N. Tian, Gold nanoparticles-based fluorescence resonance energy transfer for competitive immunoassay of biomolecules, Analyst 137 (2012) 5885–5890.
[28] L. Zhang, J.P. Lei, L. Liu, C.F. Li, H.X. Ju, Self-assembled DNA hydrogel as switchable material for aptamer-based fluorescent detection of protein, Anal. Chem. 85 (2013) 11077–11082.
[29] Y. Geng, D.J. Lin, L.J. Shao, F. Yan, H.X. Ju, Cellular delivery of quantum dot-bound hybridization probe for detection of intracellular pre-microRNA using chitosan/poly(γ-glutamic acid) complex as a carrier, Plos One 8 (2013) e65540.